HIFU Transducer Characterization Using a Robust Needle Hydrophone

Samuel M. Howard and Claudio I. Zanelli

Onda Corporation, 592 E. Weddell Drive
Sunnyvale, CA, 94089 USA

Abstract. A robust needle hydrophone has been developed for HIFU transducer characterization and reported on earlier [1]. After a brief review of the hydrophone design and performance, we demonstrate its use to characterize a 1.5 MHz, 10 cm diameter, F-number 1.5 spherically focused source driven to exceed an intensity of 1400 W/cm^{2}at its focus. Quantitative characterization of this source at high powers is assisted by deconvolving the hydrophone's calibrated frequency response in order to accurately reflect the contribution of harmonics generated by nonlinear propagation in the water testing environment. Results are compared to measurements with a membrane hydrophone at 0.3% duty cycle and to theoretical calculations, using measurements of the field at the source's radiating surface as input to a numerical solution of the KZK equation.

Keywords:Hydrophone, HIFU, cavitation, KZK
PACS: 43.35.Yb

INTRODUCTION

As previously described [1], the authors have designed a needle hydrophone that is robust in HIFU fields. Briefly, as shown in Figs 1-2, the design (referred to as the HNA hydrophone) consists of a miniature piezoceramic sensing element encased in a metallic coating twenty to seventy microns thick. The coating process was developed to provide a smooth outer surface to minimize nucleation sites for cavitation, and the coating thickness is chosen to preserve the hydrophone's acoustic response while providing a level of "blast protection". This effective diameter is within 10% of the geometric diameter of 400 μm.

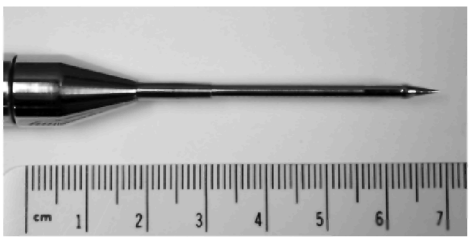

FIGURE 1. Device as built

CP911, *6th International Symposium on Therapeutic Ultrasound*
edited by C.-C. Coussios and G. ter Haar

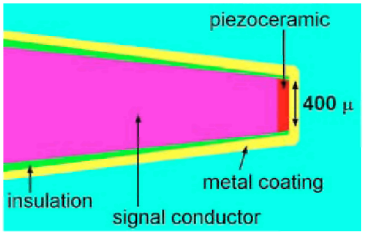

FIGURE 2. FEA model

Fig. 3 shows a typical calibrated frequency response, obtained by the authors via broadband comparison to a membrane hydrophone calibrated by National Physical Laboratory in the UK [2]. As demonstrated by Fig. 3 and discussed in [1], the hydrophone exhibits a non-flat frequency response, which increases roughly linearly from 1 to 3 MHz by about 4 dB, flattens out between 3 and 8 dB, and then dips down till approximately 15 MHz, where it rises again. The curve continues to rise until approximately 27 MHz where the ceramic has a resonance (not shown in Fig. 3, but verified by modeling and experimentally corroborated in electrical impedance measurements and in the data presented later in this paper).

A critical question is the accuracy of the HNA, given the "non-flatness" of its frequency response and the high-harmonic content of HIFU fields. This paper describes a test case where we examined this issue by comparing the measured output of an HNA to that of a much flatter membrane hydrophone (HMB-0200 manufactured by Onda Corporation, whose calibration is also shown in Fig. 3), which, while not as robust as the HNA, was put briefly put at risk in a high pressure, low duty cycle field in order to provide a comparison. In an attempt to further validate the measurements, we also compare them to predictions of a numerical solution o the KZK equation [3].

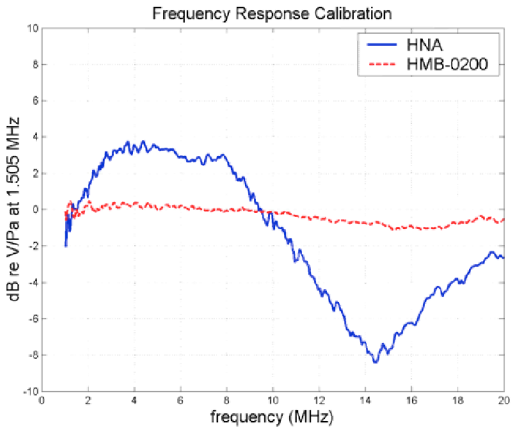

FIGURE 3. Sensitivity calibration of the HNA and HMB hydrophones used in this study, normalized by their respective sensitivities at driving frequency (147.9 mV/MPa for the HMB, and 56.6 mV/MPa for the HNA).

EXPERIMENT

The setup consisted of a HIFU source manufactured by the authors (1.505 MHz, 100 mm diameter, nominally150 mm focus, with 50 ohm impedance) in a tank of degassed, deionized water. The source transducer was driven by an HP 3314A function generator, through an ENI 240L power amplifier. It was found that the ENI amplifier started to saturate above 160 Vpp output, so 70 W was the maximum input power to the transducer in this experiment.

After aligning the axis of the hydrophone (either the HMB or HNA) to the beam axis, the measurement depth was set to 155.4 mm, as this provided the peak hydrophone signal when the source transducer was driven at maximum voltage. In order to protect the HMB, a 45 cycle, 100 Hz tone burst (i.e., 0.3% duty factor) was used. This allowed the pulse to reach a steady state within 25 :sec, at which point eight or more cycles of steady-state response could be captured. For consistency, the HNA was tested under the same conditions, although it has been found to survive with the same transducer and driving voltage at much higher duty factors—e.g., up to 40 minutes with a 50% duty factor and a 1sec repetition period. After the measurements, the hydrophones were re-inserted in the calibration setup, and the curves of Fig. 3 were duplicated to within the repeatability of the setup (approximately 2%) which confirmed that the hydrophones were not damaged.

Fig. 4(a) shows the waveforms measured at maximum power for both the HNA and the HMB, scaled by the hydrophones' calibrated sensitivities at the fundamental driving frequency of 1.505 MHz. The agreement in rarefactional pressure is good, although the HNA shows a double peak at a time separation which corresponds to the ceramic's 27 MHz resonance.

Fig. 4(b) shows that the agreement between the HNA and the membrane may be improved by deconvolving the measured calibration curves shown in Fig. 3. Because a measurement of the phase response is not currently available, the deconvolution was for the amplitude variation only. Also, the spectral response of the HNA above 20 MHz was set to zero in order to eliminate the 27 MHz resonance, and resulting truncation error is probably a cause of the oscillations in the deconvolved waveform. Nevertheless, the agreement is improved.

COMPARISON WITH A MODEL

As a further check on the results, we employed a numerical solution [4] of the time domain version of the KZK equation [3] which describes the propagation of the nonlinear wave from the source, assuming axial symmetry. The solution code requires knowledge of the source radius and curvature, as well as the radial distribution of pressure. For simplicity, and because scans of the beam near the transducer face indicated a fairly uniform beam, we chose to assume an axisymmetric uniform pressure distribution across a perfectly spherical shell. We then determined the effective radius and curvature by choosing the values that gave the best-fit to O'Neil's linear model for the axial pressure distribution around the focal zone. To make sure

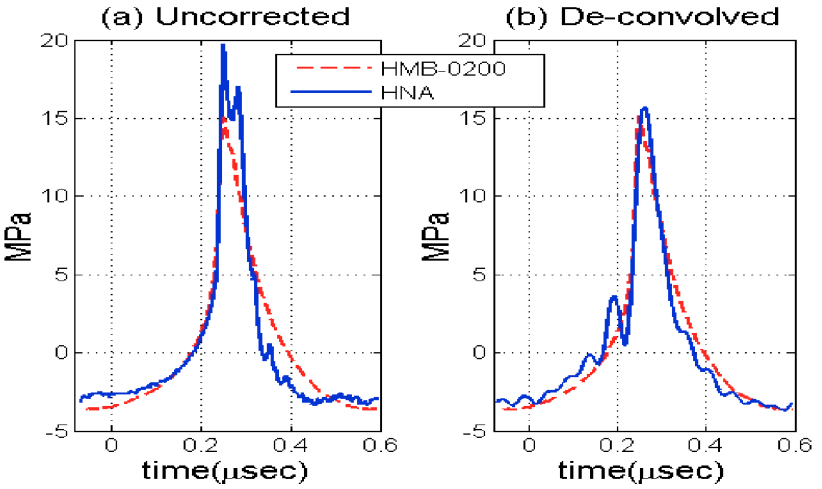

FIGURE 4. Single cycle of pressure waveform at focus. (a): HNA and HMB-0200 voltage waveforms scaled by their respective sensitivities at 1.505 MHz. (b): Data corrected by amplitude deconvolution using the calibration data shown in Fig. 3.

we performed this measurement in the linear range, the transducer was operated at a low voltage of 8Vpp (0.16 W)—at this operating voltage, the focal pressure was 308 kPa (peak) and varied within 3% of linear when the voltage was doubled. The resulting axial measurements made under these conditions were best fit by a geometric focus of 154.2mm (compared with the nominal 150 mm) and an effective radius of 49.0 mm (compared to the nominal radius of 50mm).

To determine the absolute pressure at the source transducer face (i.e. "input pressure" in terms of the model) the total power was measured with the HNA at 8Vpp input, and this was divided by the effective area of the source to determine the input intensity, and hence the average input pressure at this minimal input voltage. The HNA was then moved to approximately 10 mm from the face of the transducer, and the variation of the pressure with input voltage was then measured, and used as a scale factor for the input pressure measured at 8Vpp, to obtain the source transducer input pressure as a function of the voltage setting.

This data (effective radius, geometric focus, and input pressure) was then loaded into the code, along with the attenuation of pure water [5]. To obtain results, the origin plane was sampled with a spatial resolution of 61.2 microns, and the time step was set to 100 time steps per cycle. A ramped tone burst was used, and the central steady-state portion of the calculations was then examined as equivalent to the cw response. A single cycle is compared to the HNA and HMB-0200 data in Fig. 5.

It is also instructive to compare the theoretical and measured waveforms in terms of their harmonic constituents, as a function of average pressure at the surface of the source. The harmonic components were calculated numerically for different source pressures, Fourier-transformed, and plotted as a function of source pressure in Fig. 6.

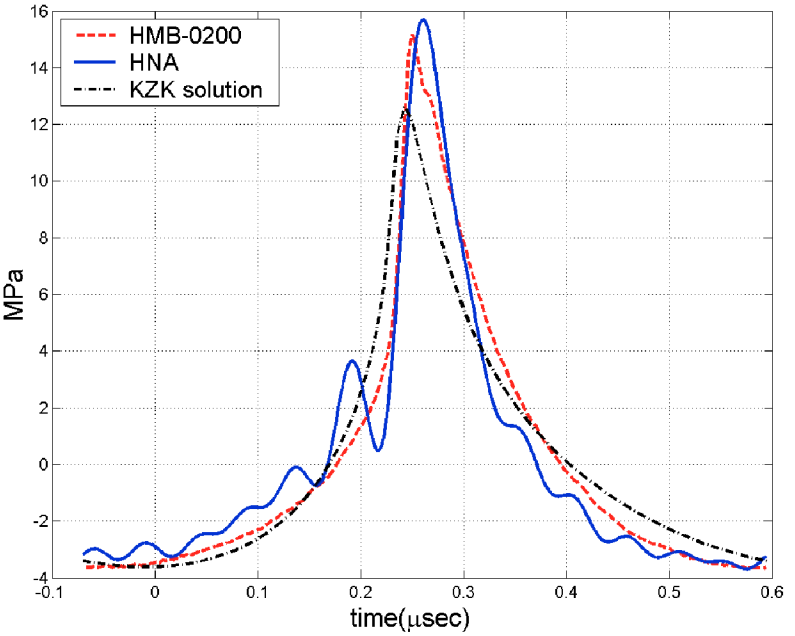

FIGURE 5. Single cycle of pressure waveform at focus. The HNA and HMB data are corrected using the sensitivity amplitude data, as in Fig. 4 (b).

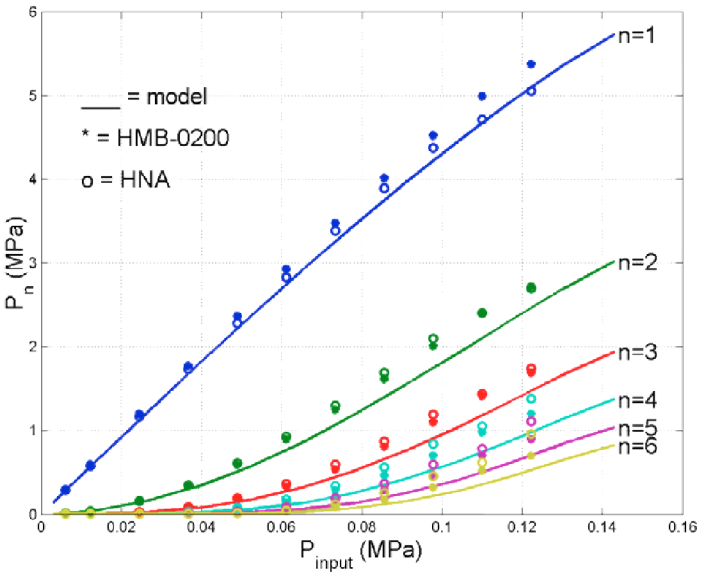

FIGURE 6. Amplitude of harmonic content of pressure waveforms as a function of average pressure across the face of the source transducer. n = 1 is the fundamental (1.505 MHz), n = 2 is 3.01 MHz, etc.

Similar data was obtained experimentally by recording waveforms at different drive voltages, Fourier-transforming them, and plotting against the input pressure estimated for each voltage setting. Only the fundamental and its first five harmonics are shown in Fig. 6, as these account for over 97% of the power in the HNA and HMB data, and for over 98% of the power in the KZK solution.

DISCUSSION

The difference between the HNA and HMB at the fundamental and its first three harmonics (n=4, or 6.02 MHz) is within 1 dB, which is estimated to be the experimental uncertainty arising from the combination of a number of error sources such as digitizer accuracy, alignment repeatability, calibration precision, etc.). Beyond the fourth harmonic, the difference between the HNA and HMB grows to almost 3 dB at the fifth harmonic (9.03 MHz) for reasons that are not yet understood.

The difference between the hydrophone data and the solution of the KZK equation is larger, and will require further study into potential error sources, including numerical error, and the errors due to assuming that the source is an ideal, uniform and axisymmetric spherical cap. Nevertheless, the authors regard the general agreement between the hydrophone data and numerical solution as reassuring

Overall, the HNA, HMB, and numerical solution are in good agreement for both the rarefactional pressure and pulse-average intensity, as shown in Table 1. The discrepancies at the higher harmonics is reflected in worse agreement in the peak pressure, although it is hoped that this metric is less clinically relevant than the rarefactional pressure and pulse-average intensity.

TABLE 1. Comparison of Waveform Metrics

	Peak Pressure (MPa)	Rarefactional Pressure (MPa)	Isppa (W/cm^2)
HNA, uncorrected	19.7	-3.4	1860
HMB, uncorrected	15.1	-3.7	1440
HNA, corrected	**15.8**	**-3.6**	**1410**
HMB, corrected	**15.1**	**-3.7**	**1430**
KZK solution	**13.0**	**-3.7**	**1250**

CONCLUSIONS

In the test case presented here, the HNA's rarefactional pressure measurement matched the membrane and KZK predictions within 10%, even without correction by deconvolving its frequency response. Deconvolution of the amplitude response provided a much closer match to the membrane hydrophone's measurements of pulse-average intensity and peak pressure—generally well within the 10% experimental errors expected. Further improvement may require an accurate phase calibration of the hydrophone, perhaps up to 30 MHz due to the 27 MHz resonance in this device.

ACKNOWLEDGEMENTS

The authors wish to thank Dr. A. Szilyagi, PhD for assistance in fabricating the hydrophone used in this study. We also thank Prof. Robin Cleveland for making the "Texas KZK code" available to the public.

REFERENCES

1. Zanelli, C I., and Howard, S. M., "A Robust Hydrophone for HIFU Metrology," Proceedings of the 5th International Symposium on Therapeutic Ultrasound, Oct. 27-29, 2005, Boston, MA, USA, pp.618-622.
2. Selfridge, A. and Lewin, P.A., "Wideband Spherically Focused PVDF Acoustic Sources for Calibration of Ultrasound Hydrophone Probes", IEEE Transactions on Ultrasonics, Ferroelectrics, and Frequency Control, Vol. 47, No. 6, November 2---, pp. 1372-1376
3. Cleveland, R. O., Hamilton, M.F. and Blackstock, D.T., "Time-domain modeling of finite-amplitude sound in relaxing fluids", J. Acoust. Soc. Am., 99(6), June 1996, pp. 3312-3318
4. "Texas KZK code" downloaded from: http://people.bu.edu/robinc/kzk/
5. O'Neil, H.T., "Theory of Focusing Radiators," J. Acoust. Soc. Am 21(5), September, 1949, pp. 516-526
6. Pierce, A.D., *Acoustics: An Introduction to its Physical Principles and Applications, McGraw-Hill, 1989, pp. 588-561.*